Application of space–time transmit diversity to single-carrier transmission with frequency-domain equalisation and receive antenna diversity in a frequency-selective fading channel

K. Takeda, T. Itagaki and F. Adachi

Abstract: In a frequency-selective fading channel, the performance of non-spread-spectrum single-carrier (SC) transmission degrades significantly due to severe intersymbol interference (ISI). The joint use of space–time transmit diversity (STTD), receive antenna diversity and frequency-domain minimum mean square error (MMSE) equalisation in non-spread SC transmission is studied. Space–time encoding and decoding for frequency-domain MMSE equalisation and receive antenna diversity is presented. The achievable bit error rate (BER) performance of non-spread SC transmission is evaluated by computer simulation. It is found that joint use of STTD, receive antenna diversity and frequency-domain MMSE equalisation can significantly improve the BER performance in a severe frequency-selective fading channel.

1 Introduction

A wireless channel is composed of many propagation paths with different time delays, producing frequency-selective multipath fading [1]. In a frequency-selective fading channel, the bit error rate (BER) performance of non-spread single-carrier (SC) transmission significantly degrades due to severe intersymbol inference (ISI). Direct-sequence code division multiple access (DS-CDMA) can exploit the channel frequency-selectivity by the use of a rake receiver that resolves the propagation paths having different time delays and coherently combines them to achieve the path diversity effect [2]. Wideband DS-CDMA has been adopted as the wireless access technique in the third generation mobile communications systems, known as IMT-2000 systems, for data transmissions of up to a few Mbit/s [3]. However, in the case of broadband wireless data transmissions of more than a few Mbit/s using DS-CDMA, the transmission performance with coherent rake combining may significantly degrade due to severe interpath interference (IPI).

Recently, multicarrier code division multiple access (MC-CDMA) has been attracting much attention for broadband wireless data transmissions in a severe frequency-selective channel [4–6]. In MC-CDMA, the frequency diversity effect is attained by one-tap frequency-domain equalisation, resulting in a better BER performance than DS-CDMA using coherent rake combining [7]. However, MC-CDMA has a problem of large peak-to-average power ratio (PAPR) and thus, a linear transmit power amplifier with a large peak power is required. Quite recently, non-spread SC transmission using one-tap frequency-domain equalisation has been gaining an increasing popularity [8]. Non-spread SC transmission has the advantages that the problem of high PAPR can be avoided and the computational complexity of frequency-domain equalisation does not depend on the degree of channel frequency-selectivity.

In this paper, we consider non-spread SC transmission with frequency-domain equalisation. Transmit/receive antenna diversity is a well known effective technique to improve the transmission performance [9]. We apply two-antenna space–time transmit diversity (STTD) [10] to further improve the BER performance of the non-spread SC transmission. Direct application of STTD of [10] involves transforming the transmit signal into the orthogonal frequency components by fast Fourier transform (FFT) and applying STTD encoding in the frequency-domain. Then, inverse FFT (IFFT) is applied to get the STTD encoded signals in the time-domain. This frequency-domain encoding allows STTD decoding to be combined with frequency-domain equalisation at the receiver. In this paper, we propose a time-domain STTD encoding that does not require FFT and IFFT operations at the transmitter. Another simple transmit diversity is the delay transmit diversity (DTD) [11]. The BER performance of non-spread SC transmission achievable with STTD combined with frequency-domain equalisation and receive antenna diversity is evaluated by computer simulation and is compared with that of DTD.

2 STTD combined with frequency-domain equalisation and receive antenna diversity

2.1 Space–time coding suitable for frequency-domain MMSE equalisation

Figure 1 illustrates the transmitter and receiver structure for non-spread SC transmission with STTD combined with frequency-domain equalisation. In this paper, we assume

IEE Proceedings online no. 20040624

doi:10.1049/ip-com:20040624

Paper first received 8th September 2003 and in revised form 13th April 2004. Originally published online: 14th October 2004

The authors are with the Adachi Laboratory, Dept. of Electrical and Communication Engineering, Graduate School of Engineering, Tohoku University, 05 Aza-Aoba, Aramaki, Aoba-ku, Sendai 980-8579, Japan

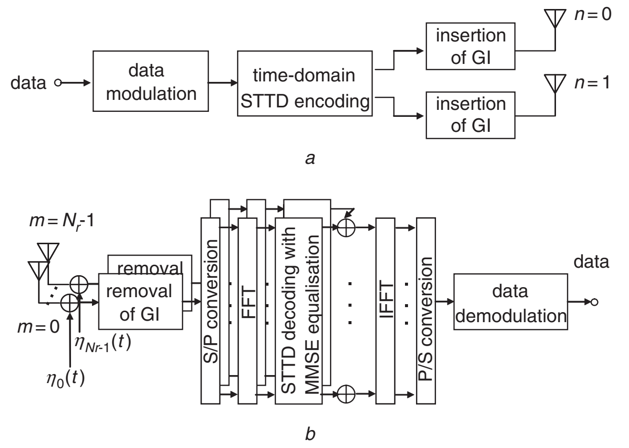

Fig. 1 *Transmitter and receiver with joint STTD, frequency-domain equalisation and receive antenna diversity*
a Transmitter
b Receiver

the square-root Nyquist pulse shaping filter at the transmitter and the same filter at the receiver as the matched filter. Also, ideal sampling timing is assumed at the receiver. In Fig. 1, square-root Nyquist filters are not shown for simplicity. Throughout the paper, discrete time representation of the signal is used.

The data symbol sequence to be transmitted is transformed into the sequence of data blocks of N_c symbols each. The N_c-data-symbol sequence of the qth block is denoted as $\{d_q(t);\ t=0\sim N_c-1\}$. The non-spread SC signal $\{s_q(t);\ t=0\sim N_c-1\}$ of the qth block is expressed using the equivalent low-pass representation as

$$s_q(t) = \sqrt{2E_s/T}\,d_q(t) \tag{1}$$

where E_s is the transmit signal energy per symbol and T is the symbol length. We extend Alamouti's STTD encoding [10] to the non-spread SC transmission using frequency-domain equalisation. The signal blocks $\{s_e(t)\}$ and $\{s_o(t)\}$ represent the even ($q=2u$) and odd ($q=2u+1$) signal blocks, respectively. Let the subcarrier components of the even ($q=2u$) and odd ($q=2u+1$) signal blocks be denoted by $\{S_e(k)\}$ and $\{S_o(k)\}$, respectively (note that non-spread SC transmission does not use subcarriers for modulation, the terminology 'subcarrier' is used for explanation purposes only). They are given by

$$\begin{cases} S_e(k) = \sum_{t=0}^{N_c-1} s_e(t)\exp\left(-j2\pi k\frac{t}{N_c}\right) \\ S_o(k) = \sum_{t=0}^{N_c-1} s_o(t)\exp\left(-j2\pi k\frac{t}{N_c}\right) \end{cases} \tag{2}$$

for $k=0\sim N_c-1$. The STTD encoding using $\{S_e(k)\}$ and $\{S_o(k)\}$ is carried out subcarrier-by-subcarrier as shown in Table 1. This frequency-domain STTD encoding allows decoding to be combined with frequency-domain equalisation (this is described in Section 2.2).

Table 1: Frequency-domain STTD encoding

Time (in block)	Antenna index n 0	1
Even ($q=2u$)	$S_e(k)$	$S_o(k)$
Odd ($q=2u+1$)	$-S_o^*(k)$	$S_e^*(k)$

The above STTD encoding requires N_c-point FFT and IFFT operations to obtain $\{S_e(k)\}$ and $\{S_o(k)\}$ and transform them back to time-domain signals, respectively. Below, an equivalent time-domain STTD encoding that requires no FFT and IFFT operations is presented. Applying N_c-point IFFT to $\{S_e^*(k)\}$and $\{S_o^*(k)\}$, we obtain

$$\begin{cases} \frac{1}{N_c}\sum_{k=0}^{N_c-1} S_e^*(k)\exp\left(j2\pi t\frac{k}{N_c}\right) = s_e^*(N_c-t) \\ \frac{1}{N_c}\sum_{k=0}^{N_c-1} S_o^*(k)\exp\left(j2\pi t\frac{k}{N_c}\right) = s_o^*(N_c-t) \end{cases} \tag{3}$$

for $t=0\sim N_c-1$, where $()^*$ denotes the complex conjugate. Hence, the STTD encoding of Table 1 can be replaced by the time-domain STTD encoding shown in Table 2, which implies that STTD encoding can be directly carried out in the time domain without applying FFT and IFFT in the transmitter. The signal blocks $\{s_e(t)\}$ and $\{s_o(t)\}$ are encoded in the time domain, as shown in Fig. 2. The last N_g symbols in each time-domain STTD encoded signal block are copied and inserted into the beginning of each block as the GI. The GI-inserted signal streams are simultaneously transmitted from two antennas over a frequency-selective fading channel.

Table 2: Equivalent time-domain STTD encoding

Time (in block)	Antenna index n 0	1
Even ($q=2u$)	$s_e(t)$	$s_o(t)$
Odd ($q=2u+1$)	$s_o^*(N_c-t)$	$s_e^*(N_c-t)$

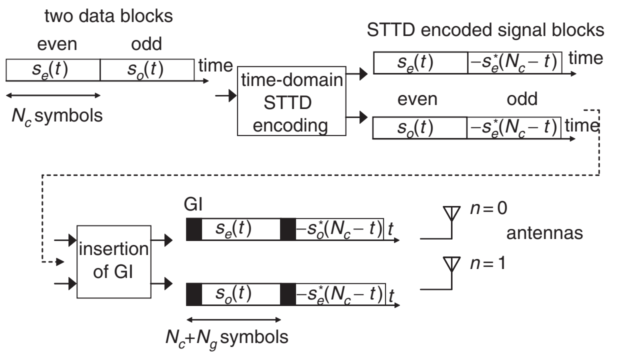

Fig. 2 *STTD encoding process for transmission from two transmit antennas*

2.2 Joint STTD decoding and frequency-domain MMSE equalisation with receive antenna diversity

The STTD encoded signal streams transmitted from two antennas are assumed to be received by N_r antennas and sampled at the symbol rate in the receiver. The propagation channel is assumed to be a symbol-spaced L-path frequency-selective fading channel, with each path subject to independent fading. Time delay τ_l of the lth path is assumed to be l symbols. Ideal channel estimation is assumed for joint STTD decoding and frequency-domain equalisation.

The signal sequences, $\{r_{e,m}(t)\}$ and $\{r_{o,m}(t)\}$, corresponding to the even and odd block time intervals, received on the mth antenna at time t can be expressed using the equivalent low-pass representation as

$$\begin{cases} r_{e,m}(t) = \frac{1}{\sqrt{2}}\sum_{l=0}^{L-1} \xi_{0,m,l} s_e(t-l) \\ \quad + \frac{1}{\sqrt{2}}\sum_{l=0}^{L-1} \xi_{1,m,l} s_o(t-l) + \eta_{e,m}(t) \\ r_{o,m}(t) = -\frac{1}{\sqrt{2}}\sum_{l=0}^{L-1} \xi_{0,m,l} s_o^*(N_c-(t-l)) \\ \quad + \frac{1}{\sqrt{2}}\sum_{l=0}^{L-1} \xi_{1,m,l} s_e^*(N_c-(t-l)) + \eta_{o,m}(t) \end{cases} \quad (4)$$

for $t=-N_g \sim N_c-1$, where $\xi_{n,m,l}$ is the lth path gain between the nth transmit antenna ($n=0,1$) and the mth receive antenna ($m=0\sim N_r-1$), and $\eta_{e,m}(t)$ and $\eta_{o,m}(t)$ represent the independent noise processes characterised by zero-mean complex Gaussian processes with variance $2N_0/T$ where N_0 is the one-sided power spectral density of additive white Gaussian noise (AWGN). Block fading, where the path gains stay constant over two (even and odd)-block interval, has been assumed. After removal of GI, the even and odd block received signal sequences are decomposed by N_c-point FFT into N_c subcarrier components $\{R_{e,m}(k);\ k=0\sim N_c-1\}$ and $\{R_{o,m}(k);\ k=0\sim N_c-1\}$, respectively. $R_{e,m}(k)$ and $R_{o,m}(k)$ can be written as

$$\begin{cases} R_{e,m}(k) = \frac{1}{\sqrt{2}}H_{0,m}(k)S_e(k) \\ \quad + \frac{1}{\sqrt{2}}H_{1,m}(k)S_o(k) + N_{e,m}(k) \\ R_{o,m}(k) = -\frac{1}{\sqrt{2}}H_{0,m}(k)S_o^*(k) \\ \quad + \frac{1}{\sqrt{2}}H_{1,m}(k)S_e^*(k) + N_{o,m}(k) \end{cases} \quad (5)$$

where $\{H_{0,m}(k)\}$ and $\{H_{1,m}(k)\}$ represent, respectively, the N_c-point Fourier transforms of the channel gains associated with the 0th and 1st transmit antennas, and $N_{e,m}(k)$ and $N_{o,m}(k)$ represent, respectively, the kth subcarrier components of $\{\eta_{e,m}(t)\}$ and $\{\eta_{o,m}(t)\}$. They are given by

$$\begin{cases} H_{n,m}(k) = \sum_{l=0}^{L-1} \xi_{n,m,l} \exp\left(-j2\pi k \frac{l}{N_c}\right), n=0,\ 1 \\ N_{e,m}(k) = \sum_{t=0}^{N_c-1} \eta_{e,m}(t) \exp\left(-j2\pi k \frac{t}{N_c}\right) \\ N_{o,m}(k) = \sum_{t=0}^{N_c-1} \eta_{o,m}(t) \exp\left(-j2\pi k \frac{t}{N_c}\right) \end{cases} \quad (6)$$

One-tap frequency-domain equalisation is carried out jointly with STTD decoding and receive antenna diversity combining to obtain $\{\tilde{S}_e(k)\}$ and $\{\tilde{S}_o(k)\}$:

$$\begin{cases} \tilde{S}_e(k) = \sum_{m=0}^{N_r-1} \left\{ w_{0,m}^*(k) R_{e,m}(k) + w_{1,m}(k) R_{o,m}^*(k) \right\} \\ \tilde{S}_o(k) = \sum_{m=0}^{N_r-1} \left\{ w_{1,m}^*(k) R_{e,m}(k) - w_{0,m}(k) R_{o,m}^*(k) \right\} \end{cases} \quad (7)$$

for $k=0\sim N_c-1$, where $w_{0,m}(k)$ and $w_{1,m}(k)$ are the STTD decoding weights. Direct application of decoding presented in [10] gives

$$\begin{cases} w_{0,m}^{(MRC)}(k) = H_{0,m}(k) \\ w_{1,m}^{(MRC)}(k) = H_{1,m}(k) \end{cases} \quad (8)$$

which are the maximal-ratio combining (MRC) weights. Another solution is that the weights are chosen so that the mean square error (MSE) between $\tilde{S}_e(k)$ and $S_e(k)$ and that between $\tilde{S}_o(k)$ and $S_o(k)$ are jointly minimised. Following [12], we can obtain the following weights:

$$\begin{cases} w_{0,m}^{(MMSE)}(k) = \dfrac{H_{0,m}(k)}{\sum_{n=0}^{1}\sum_{m=0}^{N_r-1}|H_{n,m}(k)|^2 + \left(\frac{1}{2}\frac{E_s}{N_0}\right)^{-1}} \\ w_{1,m}^{(MMSE)}(k) = \dfrac{H_{1,m}(k)}{\sum_{n=0}^{1}\sum_{m=0}^{N_r-1}|H_{n,m}(k)|^2 + \left(\frac{1}{2}\frac{E_s}{N_0}\right)^{-1}} \end{cases} \quad (9)$$

where E_s/N_0 is the average received signal energy per symbol-to-AWGN power spectrum density ratio per receive antenna. Removing the second term in the denominator of (9) leads to the zero-forcing (ZF) weights:

$$\begin{cases} w_{0,m}^{(ZF)}(k) = \dfrac{H_{0,m}(k)}{\sum_{n=0}^{1}\sum_{m=0}^{N_r-1}|H_{n,m}(k)|^2} \\ w_{1,m}^{(ZF)}(k) = \dfrac{H_{1,m}(k)}{\sum_{n=0}^{1}\sum_{m=0}^{N_r-1}|H_{n,m}(k)|^2} \end{cases} \quad (10)$$

Substitution of (8)–(10) into (7) gives

$$\begin{cases} \tilde{S}_e(k) = \frac{1}{\sqrt{2}}\tilde{H}(k)S_e(k) + \tilde{N}_e(k) \\ \tilde{S}_o(k) = \frac{1}{\sqrt{2}}\tilde{H}(k)S_o(k) + \tilde{N}_o(k) \end{cases} \quad (11)$$

where

$$\tilde{H}(k) = \begin{cases} \sum_{n=0}^{1}\sum_{m=0}^{N_r-1}|H_{n,m}(k)|^2, & \text{for MRC} \\ \dfrac{\sum_{n=0}^{1}\sum_{m=0}^{N_r-1}|H_{n,m}(k)|^2}{\sum_{n=0}^{1}\sum_{m=0}^{N_r-1}|H_{n,m}(k)|^2 + \left(\frac{1E_s}{2N_0}\right)^{-1}}, & \text{for MMSE} \\ 1, & \text{for ZF} \end{cases} \quad (12)$$

is the equivalent channel gain after STTD decoding, frequency-domain equalisation and receive antenna diversity combining, and $\tilde{N}_e(k)$ and $\tilde{N}_o(k)$ are the noise components. It can be understood from (12) that the use of STTD doubles the equivalent number of receive antenna diversity branches, i.e. $2N_r$, but, with 3 dB power penalty (this is because the transmit power from each antenna is half of that with a single transmit antenna to keep the total transmit power from two antennas the same).

N_c-point IFFT is applied to $\{\tilde{S}_e(k)\}$ and $\{\tilde{S}_o(k)\}$ to obtain the time-domain soft decision sample sequences for succeeding data demodulation.

3 Simulation results

The average BER performance of non-spread SC transmission with joint STTD, frequency-domain equalisation and receive antenna diversity is evaluated by computer simulation. The simulation parameters are given in Table 3. Quaternary phase shift keying (QPSK) data modulation, $N_c=256$, $N_g=32$ and a symbol-spaced L-path frequency-selective block Rayleigh fading having an exponential power delay profile $\Omega(\tau)$ with decay factor α are assumed. $\Omega(\tau)$ where τ is the time delay in symbols is expressed as

$$\Omega(\tau) = \sum_{l=0}^{L-1} \Omega_l \delta(\tau - l) \quad (13)$$

where $\Omega_l = E[|\xi_{n,m,l}|^2]$ for all n and m and is given by $\Omega_l = \Omega_0 \exp(-\alpha l)$.

Table 3: Simulation parameters

Transmitter	Modulation	QPSK
	Number of FFT points	$N_c = 256$
	GI	$N_g = 32$(symbols)
	Transmit diversity	STTD
Channel	Fading	frequency-selective block Rayleigh fading
	Power delay profile	$L = 16$-path exponential power delay profile decay factor $\alpha = 0,2,8,\infty$ (dB)
Receiver	Number of receive antennas	$N_r = 1,2,4$
	Frequency-domain equalisation	MMSE, MRC, ZF
	Channel estimation	ideal

The average BER performance curves shown in the following Figures are obtained by Monte Carlo simulation. At the transmitter, 10 million bits are generated for QPSK data modulation. Then, QPSK modulated symbol sequence is STTD-encoded in the time-domain as shown in Table 2. The path gain $\xi_{n,m,l}$ characterised by zero-mean complex Gaussian process is generated using Jakes model [1] having 64 plane waves. At the receiver, the zero-mean complex Gaussian noise process generated by the Box–Muller method [13] is added to the received signal sequence. The N_c-point Fourier transforms of the channel gains $H_{0,m}(k)$ and $H_{1,m}(k)$ are computed using (6). Joint STTD decoding and frequency-domain equalisation is carried out using (7). Finally, data demodulation is carried out and the BER is measured. This transmission and reception procedure, with 10 million bits each, is repeated at least 10 times to compute the average BER for the given average E_s/N_0 per receive antenna.

3.1 BER performance evaluation

The improvement in average BER performance obtained when STTD is combined with frequency-domain MRC, MMSE or ZF equalisation is discussed. Figure 3 plots the average BER performance as a function of the average signal energy per information bit-to-AWGN power spectrum density ratio E_b/N_0, which is given by $E_b/N_0 = (1 + N_g/N_c)(E_s/N_0)$, for different values of the decay factor α. When $\alpha = \infty$ dB, the channel becomes frequency-nonselective and thus, MMSE, ZF and MRC equalisations should provide the same BER performance because of the flat fading channel. This is seen in Fig. 3. However, when the channel is frequency-selective (i.e. $\alpha \to 0$ dB), MMSE equalisation gives a better BER performance than MRC and ZF equalisations. With MRC equalisation, BER floors are seen when $\alpha = 0$, 2 and 8 dB due to the severe ISI produced by the enhanced frequency-selectivity, while the BER performance of ZF equalisation is almost insensitive to the value of α. MMSE equalisation can suppress the noise enhancement while can almost restore the frequency non-selective channel. Hence, irrespective of the channel frequency-selectivity, the BER performance with MMSE equalisation is always better than with ZF equalisation. In the following, we use the MMSE equalisation only.

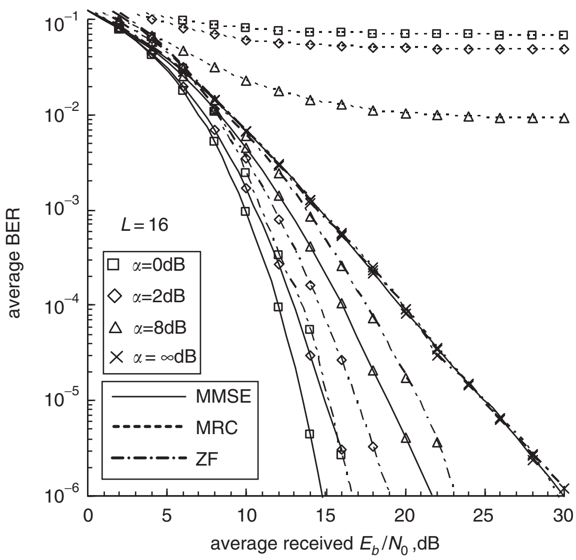

Fig. 3 *Simulated BER performance with joint STTD and MMSE, MRC or ZF equalisation*
No antenna diversity ($N_r = 1$)

The BER performance with and without STTD is compared in Fig. 4, with the decay factor α as a parameter. Since frequency-domain MMSE equalisation can achieve frequency diversity effect by taking advantage of a frequency-selective fading, $\alpha = 0$ dB gives a better BER performance than $\alpha = 8$ dB. Joint STTD and frequency-domain MMSE equalisation further improves the BER performance. An STTD gain of 4 dB at BER $= 10^{-4}$ is obtained when $\alpha = 0$ dB.

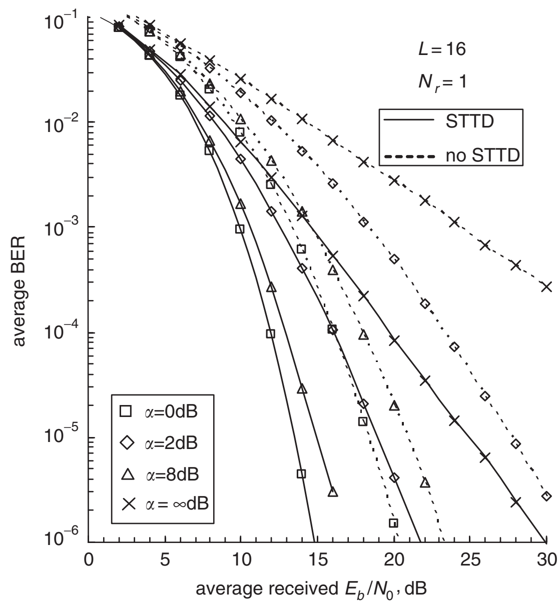

Fig. 4 *BER performance with joint STTD and MMSE equalisation*
No antenna diversity ($N_r = 1$)

An additional use of receive antenna diversity can further improve the BER performance. Figure 5 plots the average BER performance as a function of the average E_b/N_0 per receive antenna with α and the number N_r of receive antennas as parameters. The use of receive antenna diversity is always beneficial irrespective of the degree of channel frequency-selectivity. When $\alpha = 0$ dB and $N_r = 2$, a combined STTD/receive diversity gain of 4.7 dB is obtained at BER $= 10^{-4}$ compared with $N_r = 1$. When $N_r = 4$, a combined STTD/receive diversity gain of as much as 8.5 dB is obtained.

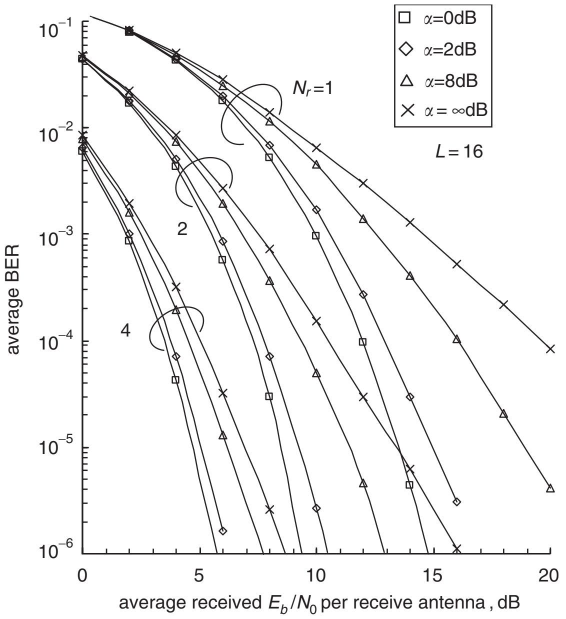

Fig. 5 *Effect of joint STTD and receive antenna diversity*

3.2 Comparison with delay transmit diversity (DTD)

We compare the BER performances achievable by STTD and DTD. Figure 6 illustrates the non-spread SC transmitter and receiver structure employing DTD. The GI-inserted signal sequence is inflicted different time delays and transmitted from N_t transmit antennas simultaneously. The time delay τ_n to be inflicted on the nth transmit antenna, $n=0\sim N_t-1$, is set as $\tau_n = n\lfloor (N_g-L)/(N_t-1)\rfloor$ symbols, where $\lfloor x \rfloor$ represents the largest integer less than or equal to x. Figure 7 illustrates the equivalent power delay profile

$$\tilde{\Omega}(\tau) = \frac{1}{N_t}\sum_{n=0}^{Nt-1}\Omega(\tau-\tau_n)$$

observed at the receiver for the case of $N_g=32$, $N_t=4$ and $\alpha=4\,\text{dB}$.

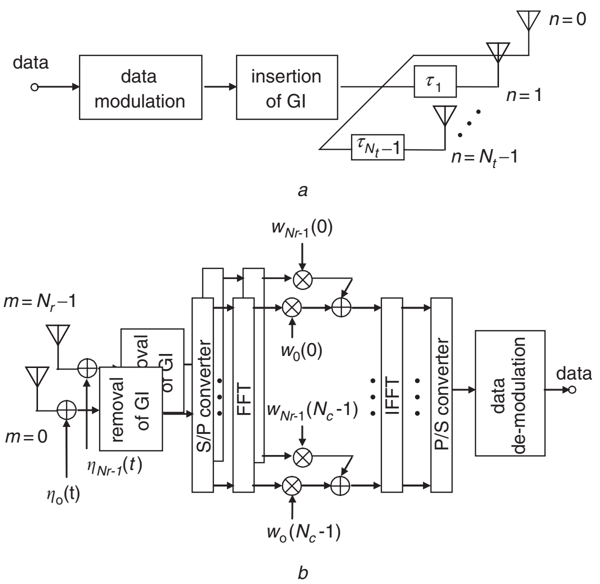

Fig. 6 *Transmitter and receiver employing DTD*
a Tranmitter
b Receiver

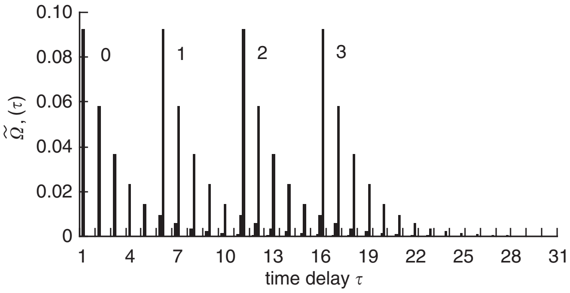

Fig. 7 *Equivalent power delay profile observed at the receiver for $N_g=32$, $N_t=4$ and $\alpha=4\,dB$*

The signal $r_m(t)$ received on the mth receive antenna at time t can be represented as

$$r_m(t) = \frac{1}{\sqrt{N_t}}\sum_{n=0}^{N_t-1}\sum_{l=0}^{L-1}\xi_{n,m,l}s_q\left(t-n\left\lfloor\frac{N_g-L}{N_t-1}\right\rfloor-l\right)+\eta_m(t) \tag{14}$$

where $\xi_{n,m,l}$ is the lth path gain between the nth transmit antenna and the mth receive antenna. After the removal of GI, the signal sequence received on the mth antenna is decomposed by N_c–point FFT into N_c subcarrier components $\{R_m(k);\ k=0\sim N_c-1\}$ and the frequency-domain MMSE equalisation is carried out as

$$\tilde{S}(k) = \frac{1}{\sqrt{N_t}}\sum_{m=0}^{N_r-1}w_m(k)R_m(k) \tag{15}$$

where $w_m(k)$ is the weight for frequency-domain MMSE equalisation and is given by [12]:

$$w_m(k) = \frac{H_m^*(k)}{\sum_{m=0}^{N_r-1}|H_m(k)|^2+\left(\frac{1}{N_t}\frac{E_s}{N_0}\right)^{-1}} \tag{16}$$

$H_m(k)$ is the channel gain observed at the kth subcarrier on the mth receive antenna and is given by

$$H_m(k) = \sum_{n=0}^{N_t-1}\sum_{l=0}^{L-1}\xi_{n,m,l}\exp\left(-\text{j}2\pi k\frac{n\left\lfloor\frac{N_g-L}{N_t-1}\right\rfloor+l}{N_c}\right) \tag{17}$$

The equivalent channel gain $\tilde{H}(k)$ after frequency-domain MMSE equalisation, corresponding to (12) for STTD, is given by

$$\tilde{H}(k) = \frac{\sum_{m=0}^{N_r-1}|H_m(k)|^2}{\sum_{m=0}^{N_r-1}|H_m(k)|^2+\left(\frac{1}{N_t}\frac{E_s}{N_0}\right)^{-1}} \tag{18}$$

Figure 8 illustrates an example of the equivalent channel gain $\tilde{H}(k)$ after frequency-domain MMSE equalisation. Since DTD increases the equivalent number of paths so as to strengthen the channel frequency-selectivity as seen in Fig. 7, a larger frequency-diversity gain can be obtained, resulting in a better BER performance.

Figure 9 compares the BER performance achievable by STTD and DTD with α as a parameter. For comparison, the BER performance for no transmit diversity is also plotted. As the channel frequency-selectivity increases (i.e. α

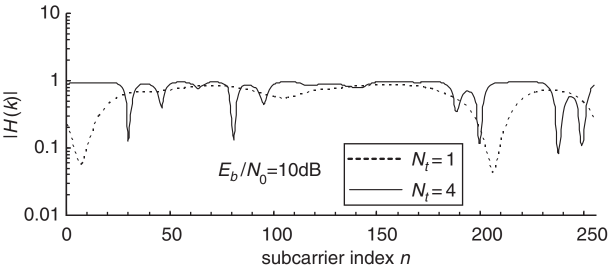

Fig. 8 *An example of $\tilde{H}(k)$ with DTD when L = 16, α = 4 dB and N_r = 1*

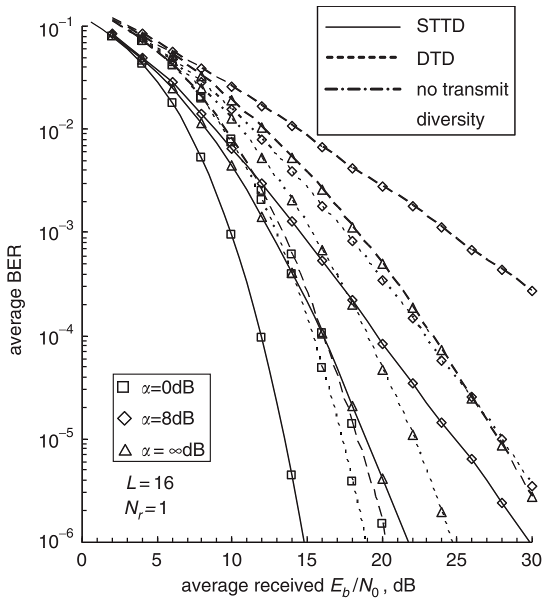

Fig. 9 *BER performance comparison for STTD and DTD*

decreases), all the BER performance for STTD, DTD and no transmit diversity improves. When $\alpha = 8$ dB, the channel frequency-selectivity becomes stronger compared to the case of $\alpha = \infty$ dB (single path) and hence, the BER performance with DTD improves. An additional gain of 3 dB at BER $= 10^{-4}$, however, is attained by STTD compared to DTD, since STTD doubles the equivalent number of receive antenna branches (see (12)). When $\alpha = 0$ dB, on the other hand, the DTD gain is only 0.7 dB because the channel frequency-selectivity is already strong enough. However, a STTD gain of as much as 3.3 dB is still obtained compared to no transmit diversity.

4 Conclusion

In this paper, STTD combined with frequency-domain equalisation and receive antenna diversity has been presented for non-spread SC transmission in a frequency-selective fading channel and the BER performance has been evaluated by computer simulation. STTD encoding suitable for frequency-domain equalisation has been proposed, in which Alamouti's STTD encoding [10] is applied to each subcarrier component (obtained by FFT) of the transmit signal sequence. The direct application of Alamouti's STTD encoding requires FFT and IFFT operations. In this paper, time-domain STTD encoding that does not require FFT and IFFT has been proposed.

Performance comparison of STTD and DTD has shown that STTD combined with frequency-domain MMSE equalisation always gives a better BER performance than DTD irrespective of the degree of channel frequency-selectivity. This is because STTD with frequency-domain MMSE equalisation is equivalent to two-branch MRC diversity while DTD expects the increased frequency diversity effect by increasing the equivalent number of propagation paths and therefore, DTD gain becomes smaller when the propagation channel frequency-selectivity is already strong enough.

In this paper, ideal channel estimation and block fading, where the channel gains stay constant over two-signal block interval, were assumed. The BER performance using practical channel estimation in a fast fading environment is left for future study. Also assumed in this paper were an ideal square-root Nyquist filter as the transmit/receive filter and ideal sampling timing. If sampling timing error is present, the intersymbol interference (ISI) is produced, resulting in degraded performance. The study of the impact of timing error is practically important and is left for future study.

5 References

1 Jakes, W.C. Jr. (Ed.): 'Microwave mobile communications' (Wiley, New York, 1974)
2 Proakis, J.G.: 'Digital communications' (McGraw-Hill, 1995, 3rd edn.)
3 Adachi, F., Sawahashi, M., and Suda, H.: 'Wideband DS-CDMA for next generation mobile communications systems', *IEEE Commun. Mag.*, 1998, **36**, pp. 56–69
4 Hara, S., and Prasad, R.: 'Overview of multicarrier CDMA', *IEEE Commun. Mag.*, 1997, **35**, pp. 126–144
5 Atarashi, H., Abeta, S., and Sawahashi, M.: 'Variable spreading factor-orthogonal frequency and code division multiplexing (VSF-OFCDM) for broadband packet wireless access', *IEICE Trans. Commun.*, 2003, **E86-B**, pp. 291–299
6 Helard, M., Gouable, R.L., Helard, J.-F., and Bandais, J.-Y.: 'Multicarrier CDMA techniques for future wideband wireless network', *Ann. Telecommun.*, 2001, **56**, (5–6), pp. 260–274
7 Sao, T., and Adachi, F.: 'Comparative study of various frequency equalisation techniques for dounlink of a wireless OFDM-CDMA system', *IEICE Trans. Commun.*, 2003, **E86-B**, pp. 352–364
8 Falconer, D., Ariyavisitakul, S.L., Benyamin-Seeyar, A., and Eidson, B.: 'Frequency domain equalisation for single-carrier broadband wireless systems', *IEEE Commun. Mag.*, 2002, **40**, pp. 58–66
9 Derryberry, R.T., Gray, S.D., Ionescu, D.M., Mandyam, G., and Raghothaman, B.: 'Transmit diversity in 3G CDMA systems', *IEEE Commun. Mag.*, 2002, **1**, pp. 68–75
10 Alamouti, S.M.: 'A simple transmit diversity technique for wireless communications', *IEEE J. Sel. Areas Commun.*, 1998, **16**, (8), pp. 1451–1458
11 Winters, J.H.: 'Diversity gain of transmit diversity in wireless systems with Rayleigh fading', *IEEE Trans. Veh. Technol.*, 1998, **47**, pp. 119–123
12 Sao, T., and Adachi, F.: 'On diversity reception of multi-rate MC-CDMA signals'. IEICE Technical Report 2002, RCS2002-204, pp. 73–78
13 Box, G.E.P., and Muller, M.E.: 'A note on the generation of random normal deviates', *Ann. Math. Stat.*, 1958, **29**, pp. 610–611